Immune landscape after allo-HSCT: TIGIT and CD161-expressing CD4 T cells are associated with subsequent leukemia relapse

Viviane Gournay, Nicolas Vallet, Vivien Peux, Kristi Vera, Jennifer
Bordenave, Marion Lambert, Aurelien Corneau, David Michonneau, Régis
Peffault de Latour, Sophie Caillat-Zucman, et al.

Immune landscape after allo-HSCT: TIGIT and CD161-expressing CD4 T cells are associated with subsequent leukemia relapse

Viviane Gournay, Nicolas Vallet, Vivien Peux, Kristi Vera, Jennifer Bordenave, Marion Lambert, Aurelien Corneau, David Michonneau, Régis Peffault de Latour, Sophie Caillat-Zucman, et al.

Immune landscape after allo-HSCT: TIGIT and CD161-expressing CD4 T cells are associated with subsequent leukemia relapse

Tracking no: BLD-2022-015522R1

Viviane Gournay (INSERM U976, France) Nicolas Vallet (INSERM U976, France) Vivien Peux (INSERM U976, France) Kristi Vera (INSERM U976, France) Jennifer Bordenave (INSERM U976, France) Marion Lambert (INSERM UMR976, France) Aurelien Corneau (Sorbonne Université, INSERM UMS037 PASS, Plateforme de Cytométrie (CyPS),, France) David Michonneau (INSERM UMR976, France) Régis Peffault de Latour (Saint-Louis, France) Sophie Caillat-Zucman (INSERM UMR976, France) Gerard Socié (INSERM UMR976, France) Mathieu Chevalier (INSERM U976, France)

Abstract:
Allogeneic hematopoietic stem-cell transplantation (allo-HSCT) is the most effective treatment for selected patients with acute myeloid leukemia (AML) and relies on a "graft-versus-leukemia" effect (GVL) where donor T lymphocytes mediate control of malignant cell growth. However, relapse remains the major cause of death after allo-HSCT. In various malignancies, several immunoregulatory mechanisms have been shown to restrain antitumor immunity, including ligand-mediated engagement of inhibitory receptors on effector cells, and induction of immunosuppressive cell-subsets such as regulatory T cells (Tregs) or myeloid-derived suppressor cells (MDSCs). While relapse after HSCT remains a major therapeutic challenge, immunoregulatory mechanisms involved in restraining the GVL effect need to be better deciphered in humans. We used mass cytometry to comprehensively characterize circulating leukocytes in two cohorts of patients after allo-HSCT. We first longitudinally assessed various immunoregulatory parameters highlighting specific trends, such as opposite dynamics between MDSCs and Tregs. More generally, the immune landscape was rather stable from month-3 to 6, while many variations occurred from month-6 to 12 post-HSCT. Comparison with healthy individuals revealed that profound alterations in the immune equilibrium persisted 1-year post-HSCT. Importantly, we found that high levels of TIGIT and CD161 expression on CD4 T cells at month 3 post-HSCT were distinct features significantly associated with subsequent AML relapse in a second cross sectional cohort. Altogether, these data provide global insights into the immunoregulatory landscape reconstitution following HSCT, and highlight non-canonical inhibitory receptors associated with relapse, which could open the path towards new prognostic tools or therapeutic targets to restore subverted anti-AML immunity.

Conflict of interest: No COI declared

COI notes:

Preprint server: No;

Author contributions and disclosures: M.F.C conceived the study, analyzed the data, and wrote the manuscript; V.G, N.V and K.V conducted the experiments and analyzed data; N.V, A.C, J.B, M.L, D.M, participated in experimental data, methodology, and editing; V.G, R.PdL and G.S provided patient samples and data; V.G, S.C-Z and G.S discussed the results and edited the manuscript.

Non-author contributions and disclosures: No;

Agreement to Share Publication-Related Data and Data Sharing Statement: Datasets can be shared without unreasonable restrictions by email to the corresponding author.

Clinical trial registration information (if any):

Immune landscape after allo-HSCT: TIGIT and CD161-expressing CD4 T cells are associated with subsequent leukemia relapse

Viviane Gournay[1,2,3], Nicolas Vallet[1,2], Vivien Peux[1,2], Kristi Vera[1,2], Jennifer Bordenave[1,2], Marion Lambert[1,2], Aurélien Corneau[4], David Michonneau[1,2,3], Régis Peffault de Latour[3], Sophie Caillat-Zucman[1,2,5], Gérard Socié[1,2,3 ✉], Mathieu F. Chevalier[1,2,✉]

1- INSERM UMR976, Human Immunology, Pathophysiology and Immunotherapy (HIPI), Paris, France.

2- Institut de Recherche Saint-Louis (IRSL), Université de Paris, Paris, France.

3- Hématologie/Transplantation, Hôpital Saint-Louis, AP-HP, Paris, France.

4- UMS037 PASS, Plateforme de Cytométrie CyPS, Faculté des Sciences, Sorbonne-Université, Paris, France.

5- Laboratoire d'Immunologie, Hôpital Saint-Louis, AP-HP, Paris, France.

✉ **Correspondence**:

Mathieu F. Chevalier, PhD
INSERM U976, Hôpital Saint-Louis,
1 Avenue Claude Vellefaux, 75010, Paris, France
E-mail: mathieu.chevalier@inserm.fr

Gérard Socié, MD, PhD
Hématologie/Transplantation, Hôpital Saint-Louis,
1 Avenue Claude Vellefaux, 75010, Paris, France
E-mail: gerard.socie@aphp.fr

Running title: Immune regulation of the GvL effect

This revised manuscript includes:
- Figures and Tables: 5 Figures and 2 Tables
- Supplemental content: 12 suppl. Figures, 3 suppl. Tables, 1 suppl. Methods

KEY POINTS

→ Immunoregulatory cell compartments show distinct dynamics and substantial persistent alterations at one year following allogeneic HSCT

→ High levels of TIGIT and CD161 expression on CD4 T cells early after allo-HSCT are associated with subsequent relapse in patients with AML

ABSTRACT

Allogeneic hematopoietic stem-cell transplantation (allo-HSCT) is the most effective treatment for selected patients with acute myeloid leukemia (AML) and relies on a "graft-versus-leukemia" effect (GVL) where donor T lymphocytes mediate control of malignant cell growth. However, relapse remains the major cause of death after allo-HSCT. In various malignancies, several immunoregulatory mechanisms have been shown to restrain antitumor immunity, including ligand-mediated engagement of inhibitory receptors on effector cells, and induction of immunosuppressive cell-subsets such as regulatory T cells (Tregs) or myeloid-derived suppressor cells (MDSCs). While relapse after HSCT remains a major therapeutic challenge, immunoregulatory mechanisms involved in restraining the GVL effect need to be better deciphered in humans. We used mass cytometry to comprehensively characterize circulating leukocytes in two cohorts of patients after allo-HSCT. We first longitudinally assessed various immunoregulatory parameters highlighting specific trends, such as opposite dynamics between MDSCs and Tregs. More generally, the immune landscape was rather stable from month-3 to 6, while many variations occurred from month-6 to 12 post-HSCT. Comparison with healthy individuals revealed that profound alterations in the immune equilibrium persisted 1-year post-HSCT. Importantly, we found that high levels of TIGIT and CD161 expression on CD4 T cells at month 3 post-HSCT were distinct features significantly associated with subsequent AML relapse in a second cross sectional cohort. Altogether, these data provide global insights into the immunoregulatory landscape reconstitution following HSCT, and highlight non-canonical inhibitory receptors associated with relapse, which could open the path towards new prognostic tools or therapeutic targets to restore subverted anti-AML immunity.

INTRODUCTION

Allogeneic hematopoietic stem cells transplantation (allo-HSCT) is the most effective consolidation treatment for patients with intermediate to high-risk acute myeloid leukemia (AML). The efficacy of allo-HSCT mostly relies on the ability of donor T cells to eliminate tumor cells, a process referred to as the graft-versus-leukemia (GVL) effect.[1-3] However, relapse still occurs in around 40% of patients and remains the main cause of mortality after allo-HSCT.[4-6] Reduced antigen presentation via HLA class-II and overexpression of ligands for inhibitory receptors (IRs) have been recently showed on relapsing AML blasts, with concomitant upregulation of IRs on T cells.[7-9] However, while research efforts have largely focused on graft-versus-host disease (GVHD), immunological mechanisms behind effectiveness of – or escape from – the GVL responses still need closer scrutiny in humans.[3,10]

Immunoregulatory mechanisms hindering efficient antitumor immune responses mainly fall into two categories: (i) cell-intrinsic, via ligand-mediated engagement of IRs expressed on effector cells (PD-1, CTLA-4, TIGIT, Tim-3, Lag-3, BTLA…), and (ii) cell-extrinsic, via immunosuppressive cell subsets, such as regulatory T cells (Tregs) or myeloid-derived suppressor cells (MDSCs).[11-13] In contrast to Tregs, a well-defined cell type described in health and diseases, MDSCs represent a more heterogeneous population (monocytic or granulocytic) known to play a major role in restraining anti-tumor T-cell responses,[12] but also possibly in limiting GVHD.[14] Other cell subsets may also exert regulatory functions in cancer contexts, such as type-2 innate lymphoid cells (ILC2).[15] Indeed, we previously identified a protumor ILC2—MDSC axis in humans[16,17] that was also associated to tolerance induction in a mouse model of GVHD.[18]

The process of immune reconstitution after allo-HSCT is slow, complex, and yet incompletely understood (reviewed in[19,20]). In contrast to early recovery of innate cells (mostly neutrophils and NK cells), the reconstitution of the adaptative system is much slower and influenced by multiple patient-, disease-, and transplant-related cofactors. Main transplant- and post-transplant cofactors influencing T- and B-cells reconstitution include recipients' age, graft source, the use of T-cell depleting agents and GVHD.[20,21] Immune reconstitution of all main immune cell subsets had been studied individually for many years by flow-cytometry, but systems-level analyses by high dimensional single cell technologies such as mass cytometry provide a wider and less biased picture of the overall process of innate and adaptative immune reconstitution.[22-24]

In this work, our aims were twofold: i) to study globally and longitudinally the immunoregulatory landscape, and ii) to identify whether and which immune cell subsets or immunoregulatory features could be associated with the emergence of subsequent relapse after allo-HSCT. As immune regulatory mechanisms involve a complex and inter-connected network of diverse immunosuppressive cells subsets and inhibitory receptors,[25] mass-cytometry was used to study circulating leukocytes following allo-HSCT in i) a longitudinal cohort up to 1 year post-HSCT, and ii) a cross-sectional cohort at month 3 post-transplant including two groups – matched for most relevant clinical variables – with patients either showing subsequent relapse or being in long-term persistent remission.

METHODS

Human biological samples

Two cohorts of HSCT recipients were studied and detailed in supplemental methods section. The first cohort included patients with AML or myelodysplastic syndrome (MDS), with pre-specified sampling at 3, 6 and 12 months post-HSCT in the absence of hematological relapse,[26,27] allowed to analyze the global longitudinal changes in the immunoregulatory landscape. The second cohort included AML patients, in which we retrospectively selected samples at 3 months post-HSCT from 20 patients who subsequently relapsed and 20 patients without relapse, matched for age at transplantation, donor type, AML cytogenetic and molecular risk.[28] Ethics approval were obtained according to French regulation (as detailed in the supplemental methods). Blood specimens were also collected from healthy volunteers (median 36 years, IQR 29-51) through the French blood bank.

Mass cytometry panel design and staining

We designed a 44 metal-labelled antibody panel as reported in Suppl. Table 1. Protocol is detailed in the supplemental methods section.

Mass cytometry data analyses and statistics

Cell events were acquired on the CyTOF Helios Mass Cytometer (Fluidigm) and data were normalized as detailed in the supplemental methods section. Data were analyzed by classical gating, as well as using the unsupervised clustering algorithms FlowSOM and UMAP for dimensional reduction.[29,30] The analyses were performed using FlowJo (v10.6), the Cytobank platform (Beckman Coulter), as well as R (v4.0.2), as detailed in the supplemental methods section. Non parametric (Mann-Whitney, Wilcoxon and log-rank) tests were used as detailed in the supplemental methods section.

RESULTS

Immunoregulatory landscape dynamics following allo-HSCT

We first aimed to comprehensively analyze longitudinal changes in peripheral immune cell subsets abundance and functional phenotype following allo-HSCT. We included 37 AML/MDS patients from the first longitudinal cohort, in whom PBMCs were collected at months 3 (M3), M6 and M12 after transplantation, as well as 20 healthy donors (**Fig. 1A**). Patients' characteristics are described in **Table 1** and Suppl. Table2. Twelve patients had relapse at a later time after sampling (particularly late with a median of 15 [IQR 8–69] months post-HSCT). Most patients with AML had intermediate or adverse factors according to the ELN classification. Relapsed patients were statistically more likely to have received a reduced intensity conditioning and not to be in complete remission at the time of transplantation. All other characteristics were similar between patients who did or did not relapse. As expected, relapsed patients had worse survival (**Table 1**).

We designed a mass-cytometry panel to assess the distribution of all main immune cell types, with a particular focus on immunoregulatory cells and receptors (i.e. Tregs, MDSCs, and a range of inhibitory

receptors). Unsupervised clustering analysis using FlowSOM (**Fig. 1B** and suppl. Fig. 1A-B) allowed identification of 121 cell clusters classified into 18 relevant metaclusters (MC) of various relative abundance (suppl. Fig. 1A). Principal component analysis revealed very distinct immune profiles in patients as compared to healthy donors, while time point after allo-HSCT did not segregate patients' samples (**Fig. 1C**).

We next tested variations of each cell cluster in paired samples at the different time points and found very few changes between M3 and M6, while frequencies of several cell clusters significantly varied from M6 to M12 (**Fig. 1D**) (detailed in suppl. Fig. 1C). At the metacluster level, we found that proportion of MC1 (hematopoietic stem/progenitor cells, HSPCs), MC2 (monocytes), MC16 (NK cells) and MC20 (CD117$^+$ ILCs) were decreasing (**Fig. 1E**), while that of MC4 (CD4 T cells), MC5 (Tregs), MC9 (Th2/Tc2 cells) and MC15 (B cells) increased over time (**Fig. 1F**). Analyses using classical manual gating strategies (suppl. Fig. 2) confirmed that only few significant changes occurred between M3 and M6 (**Fig. 1G**), while several immune parameters varied between M6 and M12 (**Fig. 1H**). Regarding immunoregulatory cell populations, all three MDSCs subsets (monocytic, granulocytic, and early-stage MDSCs[31]) were elevated in patients at M3, as compared to healthy donors (suppl. Fig. 3). Of note, the frequency of e- and M-MDSCs subsets decreased from M6 to M12 (**Fig. 1H**). In contrast, Tregs frequencies among PBMCs increased, as a reflect of increased total CD4 T cells. More specifically, only memory (CD45RA^{neg}) – both "activated" (HLA-DR$^+$) and "cytokine-secreting" (HLA-DR^{neg})[32,33] – but not naïve/resting Tregs significantly increased at M12 (**Fig. 1H**). Besides, the proportion of cells expressing the TIGIT inhibitory receptor significantly increased from M6 to M12, not only among CD8 T$_{CM}$ cells, but also among γδ-T and NK cells (**Fig. 1H**). There was also an increase in BTLA positivity on T cell subsets at M12 when compared to M3 (suppl. Fig. 4). Expression of the other inhibitory receptors (PD-1, LAG-3, Tim-3 and CTLA-4) did not significantly change over time.

Although limited by patient numbers, subgroup analyses with clinical parameters suggest an impact of ATG serotherapy in the longitudinal study of the CD4 T cell compartment (lower frequencies of CD4 T cells up to M12 in patients with ATG infusion) (suppl. Fig. 5) and of CMV reactivation on CD8 T and B cell relative abundance (suppl. Fig. 6).

Persistent alterations at 1 year after allo-HSCT

We then investigated whether and how the circulating immunoregulatory landscape remained altered one year after transplantation, when compared to the immune equilibrium at homeostasis. Hence, we first identified cell metaclusters with significantly different relative abundance between patients at M12 and healthy donors (**Fig. 2A-B**). This showed reduced relative levels of MC1 (HSPCs), MC4 (CD4 T cells), MC6 (DCs), MC13 (MAIT and other TCR Vα7.2$^+$ cells), MC14 (pDCs) and MC20 (CD117$^+$ ILCs), and elevated relative levels of MC16 (NK cells) in patients compared to healthy donors. We then generated a global atlas of each immune parameters found to be reduced (**Fig. 2C**, left panel) or elevated (**Fig. 2C**, right panel) in patients at M12. Of 203 parameters, 77 (38%) were increased and 45 (22%) decreased in transplant recipients (as shown in **Fig. 2C**) thus emphasizing profound and diverse persistent alterations in the immune equilibrium in transplant recipients. As summarized in **Fig. 2D**, these analyses confirmed long-term delayed relative reconstitution of CD4 T cells, MAIT cells, pDCs, non-classical monocytes and of the three subsets of innate lymphoid cells (ILC1, ILC2, and ILC3/P), in contrast to the immature (CD56^{bright}CD16^{neg}) NK cells that were overrepresented in patients. Moreover, the T-cell compartment

was biased toward the effector memory (EM) and terminally differentiated (TEMRA) phenotype, mirrored by a persistent lower frequency of naïve and central memory (CM) T cells. Of note, the intracellular cytotoxic molecule Granzyme B was expressed at higher levels in most T cell subsets, as well as in NK cells. Regarding immunoregulatory cell populations, MDSCs only partly normalized with persistently elevated relative levels of cells with phenotype of e- and G-MDSCs, while M-MDSC levels were similar to those of healthy donors. Total Treg frequency was also similar in patients and healthy donors, but the Treg compartment was biased toward activated (CD45RA^{neg}HLA-DR$^+$) Tregs. Importantly, most inhibitory receptors (TIGIT, PD-1, Tim-3, LAG-3, CTLA-4) as well as the immunoregulatory ectoenzyme CD39 were expressed on a higher proportion of CD8 and/or CD4 T cells and NK cells from patients (**Fig. 2B-C**). Surprisingly, the opposite was observed for the BTLA inhibitory receptor, that was expressed at lower frequencies on T cells from patients. This may reflect the above-mentioned deficiency in naïve T cells in patients, as BTLA downregulation is a known feature of T-cell differentiation.[34]

Identification of an immune profile associated with subsequent late relapse

In this longitudinal cohort, late AML/MDS relapse occurred in 12 patients (median 15 months post-HSCT). We investigated whether the immunoregulatory profile showed particular features in these patients with late relapse compared to those in long-term persistent remission (median follow-up 9.8 [IQR 8.3–9.9] years). When assessed at M3, frequencies of naïve/CM CD8 T cells and γδ T cells were found at higher levels in patients with persistent remission (with only 9 patients of the relapsing group available at this time point) (suppl. Fig. 7A). We then compared immune parameters at the M12 (or last available) time point, and found a slight segregation between patients with or without subsequent tumor relapse in a principal component analysis (PCA) (**Fig. 3A**). Most metaclusters were found at similar relative levels between both groups (suppl. Fig. 7B). However, frequencies of MC18 (γδ T cells) and MC13 (MAIT cells) were significantly decreased in patients with subsequent relapse as compared to those with sustained remission (**Fig. 3B**). Among all single immune parameters differing between both patient groups (**Fig. 3C**), we identified that increased proportions of all innate-like T cell subsets (MAIT, γδ T and NKT cells) and of naïve CD8 T cells were associated with long-term remission. Notably, frequencies of TIGIT-expressing cells were increased among various T-cell subsets in patients with subsequent relapse (**Fig. 3C**).

Cross-sectional cohort study reveals T-cell subsets associated to subsequent AML relapse

The first cohort had substantial limitations to study immune parameters associated to relapse (few and only late relapses, disease heterogeneity, no matching for confounding risk factors). We thus next investigated a homogenous retrospective cohort including 40 patients at M3 post-transplant (**Fig. 4A**). Patients' characteristics are described in **Table 2** and Suppl. Table2. Twenty patients with AML relapse (after M3, median 8.7 months) and 20 patients without documented relapse (median follow-up 32 [IQR 17–52] months) were matched according to known disease relapse risks, as described in the method section. All other parameters were similar between both groups, with only non-significant higher risk of subsequent chronic GVHD, and, as expected, worse survival in relapsing patients (**Table 2**). We first performed a FlowSOM analysis of all PBMCs from all patients and including 28 subsets-defining phenotypic markers (suppl. Fig. 8). In this well-matched cohort, we found no difference between both patient groups in the frequency of any FlowSOM-generated cell clusters (data not shown). We next

focused on the T-cell compartment and performed an ad hoc FlowSOM analysis of pre-gated total T-cells (**Fig. 4B**), with all functional markers included for the cluster generation (suppl. Table 1). While none of the clusters was enriched in non-relapsing patients, three CD4 T-cell clusters (C25, C26, C22) and one rare CD8 T-cell cluster (C79) were found at increased frequencies in patients with subsequent relapse (**Fig. 4C-D**). In comparison to bulk CD4 or CD8 T cells, all of these cell clusters expressed higher surface levels of several inhibitory receptors, and higher CD39 expression (for C25 and C26) (**Fig. 4E**).

CD161 and/or TIGIT are peculiar features of T-cell clusters associated to subsequent relapse

We then further deciphered what distinguished relapse-associated T-cell clusters from bulk CD4 or CD8 T cells. All of the identified clusters expressed PD-1, as well as at least one of the following receptors: TIGIT (C25, C26, C79), BTLA (C25, C26), and/or CD161 (C26, C22) (**Fig. 4F-G**). To highlight specific features, we measured the enrichment in frequency or density of inhibitory receptors expression on the clusters versus bulk CD4 (**Fig. 4H**) or CD8 (**Fig. 4I**) T cells. Notably, while PD-1 was expressed on all cells of the four identified cell subsets, it was only poorly enriched due to substantial PD-1 expression on other T cells not associated to tumor relapse. In contrast, cell clusters had stronger enrichment in either TIGIT (C25, C26) and/or CD161 (C26, C22) expression, both when measured as frequency of positive cells or as expression density (**Fig. 4H-I**). Thus, TIGIT and/or CD161 expression appeared the most distinguishable features of T-cell clusters (non-MAIT) enriched in relapsing patients. Accordingly, higher levels of TIGIT$^+$ (C25+26), as well of CD161$^+$ (C26+22) CD4 T-cell clusters at M3 post-transplant were associated with shorter AML relapse-free survival (**Fig. 4J**).

CD4 T cells expressing the non-canonical CD161 inhibitory receptor differ from cells with classical exhaustion phenotype and are strongly associated with poor relapse-free survival

Interestingly, CD161 was recently described as a novel inhibitory receptor restraining anti-tumor T cells in the context of malignant glioma where tumor cells expressed the CD161 ligand CLEC2D.[35] Notably, in an ad-hoc transcriptomic analysis using the *TCGA Pan-Cancer Atlas Studies* on cBioPortal,[36] we found that AML ranked third out of the 35 cancer types with regard to CLEC2D expression levels (suppl. Fig. 9).

Based on the results from the unsupervised clustering analysis described above, we next sought to further characterize total CD161$^+$ but also TIGIT$^+$ cells by classical gating in non-Treg CD4 T cells from healthy donors and patients of the cross-sectional cohort (**Fig. 5A**). PD-1$^+$ CD4 T cells were also studied as comparison. Albeit CD161 is highly expressed on MAIT cells, the analysis of CD161$^+$ CD4 T cells did not include MAITs which are almost all CD4^{neg} (CD8$^+$ or double-negative).

First, we found in a Boolean analysis that frequencies of CD4 T cells in patients at M3 post-HSCT expressing i) CD161$^+$, ii) TIGIT$^+$, as well as iii) at least TIGIT and/or CD161, were significantly elevated in subsequently relapsing patients (**Fig. 5B**), while only a trend was observed for PD-1$^+$ CD4 T cells. Of note, comparison to healthy donors showed that CD161 and TIGIT expression were upregulated in patients (**Fig. 5B**) and remained stably elevated throughout the 1-year follow-up in the first longitudinal cohort (suppl. Fig. 10). However, CD161 upregulation (median 1.3-fold increase vs healthy donors) was modest in comparison to the more markedly elevated expression of TIGIT (2.2-fold increase) and PD-1 (2.5-fold increase). Interestingly, UMAP embedding of CD4 T cells showed that CD161$^+$ T cells poorly overlapped with TIGIT$^+$ cells, that rather clustered within PD-1-expressing cells (**Fig. 5C**). Accordingly, TIGIT$^+$ cells expressed higher levels of the other inhibitory receptors PD-1 and BTLA (**Fig. 5D**), and even higher PD-1

density than total PD-1$^+$ cells themselves. Furthermore, TIGIT$^+$ but not CD161$^+$ cells were significantly enriched in dividing cells (intranuclear Ki-67 positivity) and in cells expressing HLA-DR, a marker of chronic T-cell activation (**Fig. 5E**). Altogether, these data suggest that CD161$^+$ cells – in contrast to TIGIT$^+$ cells – exhibit a profile that is rather distinct from the classical exhaustion phenotype.

We then determined whether levels of CD161$^+$ or TIGIT$^+$ CD4 T cells may vary depending on various clinical parameters, including conditioning regimen, donor type, GVHD and CMV reactivation. Notably, no significant difference was observed for most parameters, except for increased frequencies of TIGIT$^+$ cells in patients transplanted from an unrelated donor and lower levels of CD161$^+$ CD4 T cells in patients with acute GVHD (**Fig. 5F**), and more specifically ≥ grade 3 aGVHD (suppl. Fig. 11).

As TIGIT expression on not only CD4 but also CD8 T cells were associated to late relapse in the longitudinal cohort, we asked whether TIGIT+ T cells were associated to relapse-free survival in the cross-sectional cohort. Notably, high TIGIT expression on CD4 T cells and on naïve – but not bulk – CD8 T cells were significantly associated with poor relapse-free survival (suppl. Fig. 12).

Finally, in light of these results raising interest in CD161-expressing CD4 T cells, we further deciphered our previously-mentioned FlowSOM clustering with phenotypical markers on bulk PBMCs (suppl. Fig. 8A) since CD161 was included as a marker for MAIT cell identification. Interestingly, the cluster C34 corresponded to the total CD161$^+$ (non-MAIT, non-γδ TCR$^+$, non-Treg) CD4 T cell population (rather than a smaller FlowSOM subcluster as identified in Figure 4). Albeit frequency among total PBMCs was not found to be related to relapse, we normalized its level to the CD4 compartment. Strikingly, high C34 cluster frequency among CD4 T cells was strongly associated to poor AML relapse-free survival (**Fig. 5G**), thus confirming the clinical relevance of CD161 expression within CD4 T cells with regard to subsequent AML relapse.

DISCUSSION

In this study, high dimensional mass cytometry allowed to comprehensively analyze the global immune reconstitution – focusing on the immunoregulatory landscape – after allo-HSCT in a total of 77 patients with myeloid malignancies. We highlighted the overall relative dynamics and persistent alterations of a large range of immunoregulatory parameters. Importantly, a second specifically designed cohort study revealed, by both classical and unsupervised clustering analysis, that TIGIT and CD161 expression on CD4 T cells were distinct early parameters strongly associated to subsequent relapse.

The first cohort allowed to globally assess the longitudinal variations in distribution and phenotypic functional states of the main immune cell compartments during the first year post-HSCT. Although there was substantial interindividual variability, the immune landscape was surprisingly stable between M3 and M6 while many significant changes occurred at M12. As previously demonstrated in studies focusing on individual cell subsets, proportion of B cells and CD4 T cells were increasing at 1-year, at the expense of monocytes and NK cells frequencies, reflecting the well-described reconstitution kinetics of these subsets.[19,20] At 1-year, there was a persistent proportional lack of naïve T cells, MAITs, ILCs (all subsets) and pDCs. Conversely, the NK cell compartment was disproportionate due to increased frequencies of cells with an immature CD56^{bright}CD16^{neg} profile. Besides, nearly all T and NK cell subsets had higher expression of Granzyme B and activation/exhaustion markers. This global approach thus highlighted that

the overall immune landscape was still largely imbalanced even 1-year post-transplant. Of note, data highlight a persistent general immune activation state, which may have implication for long-term risk of cardiovascular comorbidities after HSCT,[37] as well described for residual chronic immune activation in treated HIV-infection.[38]

Regarding regulatory cell subsets, we found opposite patterns in Tregs and MDSCs dynamics. As other CD4 T cells, Tregs frequencies increased and were biased toward the activated phenotype at 1-year post-HSCT. In line with previous studies, this may reflect the followings: i) thymic generation of Tregs, compared to other CD4 T cells, is markedly impaired after HSCT, so that Tregs in this context mostly expand by lymphopenia-driven homeostatic proliferation,[39] and ii) naïve Tregs have a strong potential to proliferate and convert to activated Tregs.[32] This may thus account for the delayed increase in total Tregs and shrinkage of the naïve Treg pool. In sharp contrast to Tregs, relative levels of monocytic, granulocytic and early MDSCs subsets were all abnormally elevated at M3 and decreased over time. Only sparse data are available about human MDSCs subsets after allo-HSCT but, in line with our results, increased M-MDSCs levels were reported in this context.[40] Of note, we found that only M-MDSCs levels normalized at 1-year, while levels of G- and e-MDSC remained significantly elevated. The inflammatory context and severe immunosuppression following HSCT conditioning may be the driving forces for MDSCs expansion favored by inflammatory cytokines (e.g. IL-6 or IL-1β) and emergency myelopoiesis.[41,42] Of note, MDSCs may also originate directly from the graft as these cells are enriched in peripheral blood grafts following G-CSF stem cell mobilization.[43] The strong and persistent lack of ILC reconstitution following allo-HSCT nearly rules out involvement of the ILC2-MDSC axis in this context.

We aimed to investigate whether immunoregulatory features after allo-HSCT may be associated with subsequent tumor relapse. In the first cohort including late relapse events, cell subsets associated with persistent remission were interestingly mostly belonging to the innate-like T cell compartment (MAIT, γδ T and NKT cells) or conventional naïve T cells. These cells mainly arise from de novo production in the thymus, which may stress the importance of the thymic function in the GVL effect. However, they all show different reconstitution dynamics and innate-like T cells may also substantially depend on the commensal microbiota.[44] These unconventional T cell subsets with (semi-)invariant TCRs may exert antitumor functions, albeit protumor roles have also been described (reviewed in[45]). Their role in the context of HSCT is currently emerging, although studies were limited by disease heterogeneity and low patient number.[44] The first cohort in the present work also showed important limitations to study disease relapse (few and only late relapse events).

We thus specifically designed a homogeneous and balanced cohort matched for important confounding risk factors. Thereby, we identified via both classical and unsupervised clustering strategies, that early TIGIT and CD161 expression on CD4 T cells are associated to subsequent leukemia relapse. Higher PD-1 expression on CD8 T cells has been reported at the time of relapse after HSCT,[7,8] which could be a cause but most probably a consequence of tumor development. However, exhausted PD-1^{+}Eomes^{+}T-bet^{neg} CD8 T$_{SCM}$ cells in the bone marrow early after transplant – as well as tumor-specific PD-1^{+} CD8 T cells – have been described in patients prone to relapse.[8] Our work confirmed that PD-1-expressing T cell clusters were associated to subsequent relapse. Nevertheless, we found that a more specific feature of T cells associated to relapse was expression of a less commonly studied (TIGIT) and a newly identified (CD161) inhibitory receptor.[35] Elevated TIGIT expression on CD8 T cells was previously reported in AML patients and corelated to poor clinical outcome.[46] Importantly, the TIGIT ligands CD155/PVR and

CD112/PVRL2 are expressed on AML blasts,[7,46,47] and percentage and/or expression density of these receptors are even increased on AML blasts at relapse post-HSCT compared to those at diagnosis. Together with our results, data argue for the involvement of TIGIT-mediated immune escape in this context.

Of note, DNAM-1 (CD226) share the same nectin(-like) ligands as TIGIT, but is conversely an activating receptor involved in T- and NK cell-mediated cytotoxicity. Interestingly, contrary to TIGIT, DNAM-1 expression is decreased on T and NK cells from AML patients.[46,48] One could hypothesize that concomitant loss of DNAM1 together with TIGIT upregulation is an exhaustion phenotype that may play a role in AML relapse, as shown in a murine model of myeloma escape after autologous HSCT.[49]

While CD161 is a classical marker for MAIT cells, unsupervised analyses unexpectedly pinpointed the clinical relevance of CD161 expression on CD4 T cells that were neither MAIT, nor Treg or γδ-T cells. Of note, CD161-expressing CD4 T cells may encompass Th17 cells may but these are rare compared to total CD161$^+$ CD4 T cells. Interestingly, CD161 was very recently described as a novel inhibitory receptor restraining anti-tumor CD8 and CD4 T cells in glioma.[35] Of note, CD161 and TIGIT expression poorly overlapped and CD161$^+$ CD4 T cells were more distinct from a classical exhaustion phenotype than TIGIT$^+$ CD4 T cells. As high level of CD161$^+$ CD4 T cells was strongly associated with poor relapse-free survival – and also with absence of severe acute GVHD –, the functional role of this molecule will deserve further investigation in this context. Importantly, the CD161 ligand CLEC2D (LLT1) showed one of the highest expression levels in AML when comparing to a large range of cancer types (including glioblastoma).

Interestingly, we found association between relapse and IR expression mostly within the CD4 T cell compartment. Notably, it was previously demonstrated that (i) MHC class-II (rather than class-I) molecules are downregulated on AML blasts at relapse versus at diagnosis,[7,9] (ii) HLA-DP mismatches reduce the risk of leukemia relapse[50] and (iii) CD4 T cells are required – and possibly sufficient – for GVL responses in murine models of donor lymphocyte infusion.[51,52] Altogether, these data suggest a crucial role for effective CD4 T cells in the GVL effect, either as cytokine-secreting helper cells but also as direct cytotoxic lymphocytes.[53]

In the present study, neither Tregs, nor any MDSCs subsets, were associated to subsequent relapse. This is of interest for strategies aiming at increasing their number to prevent or treat GVHD while preserving the GVL effect. Indeed, besides ongoing effort on Treg cell therapies, MDSCs were also found to inhibit GVHD in preclinical models,[54] and ILC2 infusion is also raising interest to induce tolerance via MDSCs induction.[18,55]

Limitations of this work include the lack of data regarding the bone marrow immunoregulatory landscape or regarding TCR repertoire diversity and T-cell metabolism that may also be of interest with regard to the GVL effect.[56-58] Moreover, this study was limited to HLA-matched transplantation to obtain a homogeneous cohort thus limiting confounding factors, but more recent approaches such as haploidentical HSCT may warrant further investigations. Notably, in the latter setting, impaired NK cell recovery after posttransplant cyclophosphamide was found to predict relapse.[59] Finally, it remains an open question what factor(s) may impact TIGIT and CD161 expression levels, which were highly heterogenous between patients but rather stable over the months. It would be of interest to assess whether these are correlated to the levels found in the corresponding graft donors.

Overall, there is now a growing body of evidence arguing for IR-mediated AML immune escape following allo-HSCT. Yet PD-1 blockade is the most commonly used immunotherapy to date, one could speculate that TIGIT and CD161 may represent more relevant targets in this context. The use of immune checkpoints-blocking antibodies may raise concerns about exacerbating GVHD, so that innovative therapeutic strategies could be required to selectively target and reinvigorate tumor- but not healthy tissue-specific alloreactive T cells.

Authorship Contributions

Contribution: M.F.C conceived the study, analyzed the data, and wrote the manuscript; V.G, V.P., N.V and K.V conducted the experiments and analyzed data; A.C, J.B, M.L, D.M, participated in experimental data, methodology, and editing; V.G, R.PdL and G.S provided patient samples and data; V.G, S.C-Z and G.S discussed the results and edited the manuscript.

Conflict of interest statement

The authors declare no competing financial interests related to this work.

REFERENCES

1.   Horowitz MM, Gale RP, Sondel PM, et al. Graft-versus-leukemia reactions after bone marrow transplantation. *Blood*. 1990;75(3):555-562.

2.   O'Neill AT, Chakraverty R. Graft Versus Leukemia: Current Status and Future Perspectives. *J Clin Oncol*. 2021;39(5):361-372.

3.   Blazar BR, Hill GR, Murphy WJ. Dissecting the biology of allogeneic HSCT to enhance the GvT effect whilst minimizing GvHD. *Nat Rev Clin Oncol*. 2020;17(8):475-492.

4.   McDonald GB, Sandmaier BM, Mielcarek M, et al. Survival, Nonrelapse Mortality, and Relapse-Related Mortality After Allogeneic Hematopoietic Cell Transplantation: Comparing 2003-2007 Versus 2013-2017 Cohorts. *Ann Intern Med*. 2020;172(4):229-239.

5.   Horowitz M, Schreiber H, Elder A, et al. Epidemiology and biology of relapse after stem cell transplantation. *Bone Marrow Transplant*. 2018;53(11):1379-1389.

6.   Barrett AJ, Battiwalla M. Relapse after allogeneic stem cell transplantation. *Expert Rev Hematol*. 2010;3(4):429-441.

7.   Toffalori C, Zito L, Gambacorta V, et al. Immune signature drives leukemia escape and relapse after hematopoietic cell transplantation. *Nat Med*. 2019;25(4):603-611.

8.   Noviello M, Manfredi F, Ruggiero E, et al. Bone marrow central memory and memory stem T-cell exhaustion in AML patients relapsing after HSCT. *Nat Commun*. 2019;10(1):1065.

9.   Christopher MJ, Petti AA, Rettig MP, et al. Immune Escape of Relapsed AML Cells after Allogeneic Transplantation. *N Engl J Med*. 2018;379(24):2330-2341.

10.   Zeiser R, Vago L. Mechanisms of immune escape after allogeneic hematopoietic cell transplantation. *Blood*. 2019;133(12):1290-1297.

11.   Fridman WH, Pages F, Sautes-Fridman C, Galon J. The immune contexture in human tumours: impact on clinical outcome. *Nat Rev Cancer*. 2012;12(4):298-306.

12.   Marvel D, Gabrilovich DI. Myeloid-derived suppressor cells in the tumor microenvironment: expect the unexpected. *J Clin Invest*. 2015;125(9):3356-3364.

13.   Togashi Y, Shitara K, Nishikawa H. Regulatory T cells in cancer immunosuppression - implications for anticancer therapy. *Nat Rev Clin Oncol*. 2019;16(6):356-371.

14.   D'Aveni M, Notarantonio AB, Bertrand A, Boulange L, Pochon C, Rubio MT. Myeloid-Derived Suppressor Cells in the Context of Allogeneic Hematopoietic Stem Cell Transplantation. *Front Immunol*. 2020;11:989.

15.   Trabanelli S, Chevalier MF, Derre L, Jandus C. The pro- and anti-tumor role of ILC2s. *Semin Immunol*. 2019:101276.

16.   Chevalier MF, Trabanelli S, Racle J, et al. ILC2-modulated T cell-to-MDSC balance is associated with bladder cancer recurrence. *J Clin Invest*. 2017;127(8):2916-2929.

17.   Trabanelli S, Chevalier MF, Martinez-Usatorre A, et al. Tumour-derived PGD2 and NKp30-B7H6 engagement drives an immunosuppressive ILC2-MDSC axis. *Nat Commun*. 2017;8(1):593.

18.   Bruce DW, Stefanski HE, Vincent BG, et al. Type 2 innate lymphoid cells treat and prevent acute gastrointestinal graft-versus-host disease. *J Clin Invest*. 2017;127(5):1813-1825.

19.   Ogonek J, Kralj Juric M, Ghimire S, et al. Immune Reconstitution after Allogeneic Hematopoietic Stem Cell Transplantation. *Front Immunol*. 2016;7:507.

20.   Velardi E, Tsai JJ, van den Brink MRM. T cell regeneration after immunological injury. *Nat Rev Immunol*. 2021;21(5):277-291.

21.   Lin RJ, Elias HK, van den Brink MRM. Immune Reconstitution in the Aging Host: Opportunities for Mechanism-Based Therapy in Allogeneic Hematopoietic Cell Transplantation. *Front Immunol*. 2021;12:674093.

22. Lakshmikanth T, Olin A, Chen Y, et al. Mass Cytometry and Topological Data Analysis Reveal Immune Parameters Associated with Complications after Allogeneic Stem Cell Transplantation. *Cell Rep*. 2017;20(9):2238-2250.

23. McGuire HM, Rizzetto S, Withers BP, et al. Mass cytometry reveals immune signatures associated with cytomegalovirus (CMV) control in recipients of allogeneic haemopoietic stem cell transplant and CMV-specific T cells. *Clin Transl Immunology*. 2020;9(7):e1149.

24. Stern L, McGuire H, Avdic S, et al. Mass Cytometry for the Assessment of Immune Reconstitution After Hematopoietic Stem Cell Transplantation. *Front Immunol*. 2018;9:1672.

25. Schneider AK, Chevalier MF, Derre L. The multifaceted immune regulation of bladder cancer. *Nat Rev Urol*. 2019.

26. Clave E, Busson M, Douay C, et al. Acute graft-versus-host disease transiently impairs thymic output in young patients after allogeneic hematopoietic stem cell transplantation. *Blood*. 2009;113(25):6477-6484.

27. Glauzy S, Soret J, Fournier I, et al. Impact of acute and chronic graft-versus-host disease on human B-cell generation and replication. *Blood*. 2014;124(15):2459-2462.

28. Dohner H, Estey E, Grimwade D, et al. Diagnosis and management of AML in adults: 2017 ELN recommendations from an international expert panel. *Blood*. 2017;129(4):424-447.

29. Van Gassen S, Callebaut B, Van Helden MJ, et al. FlowSOM: Using self-organizing maps for visualization and interpretation of cytometry data. *Cytometry A*. 2015;87(7):636-645.

30. Becht E, McInnes L, Healy J, et al. Dimensionality reduction for visualizing single-cell data using UMAP. *Nat Biotechnol*. 2018.

31. Bronte V, Brandau S, Chen SH, et al. Recommendations for myeloid-derived suppressor cell nomenclature and characterization standards. *Nat Commun*. 2016;7:12150.

32. Miyara M, Yoshioka Y, Kitoh A, et al. Functional delineation and differentiation dynamics of human CD4+ T cells expressing the FoxP3 transcription factor. *Immunity*. 2009;30(6):899-911.

33. Dong S, Maiella S, Xhaard A, et al. Multiparameter single-cell profiling of human CD4+FOXP3+ regulatory T-cell populations in homeostatic conditions and during graft-versus-host disease. *Blood*. 2013;122(10):1802-1812.

34. Derre L, Rivals JP, Jandus C, et al. BTLA mediates inhibition of human tumor-specific CD8+ T cells that can be partially reversed by vaccination. *J Clin Invest*. 2010;120(1):157-167.

35. Mathewson ND, Ashenberg O, Tirosh I, et al. Inhibitory CD161 receptor identified in glioma-infiltrating T cells by single-cell analysis. *Cell*. 2021;184(5):1281-1298 e1226.

36. Gao J, Ciftci E, Raman P, et al. The cBioPortal for Cancer Genomics: an open source platform for accessing and interpreting complex cancer genomics data in the era of precision medicine. *Cancer Research*. 2017;77.

37. Rovo A, Tichelli A, Late Effects Working Party of the European Group for B, Marrow T. Cardiovascular complications in long-term survivors after allogeneic hematopoietic stem cell transplantation. *Semin Hematol*. 2012;49(1):25-34.

38. Zicari S, Sessa L, Cotugno N, et al. Immune Activation, Inflammation, and Non-AIDS Co-Morbidities in HIV-Infected Patients under Long-Term ART. *Viruses*. 2019;11(3).

39. Matsuoka K, Kim HT, McDonough S, et al. Altered regulatory T cell homeostasis in patients with CD4+ lymphopenia following allogeneic hematopoietic stem cell transplantation. *J Clin Invest*. 2010;120(5):1479-1493.

40. Mougiakakos D, Jitschin R, von Bahr L, et al. Immunosuppressive CD14+HLA-DRlow/neg IDO+ myeloid cells in patients following allogeneic hematopoietic stem cell transplantation. *Leukemia*. 2013;27(2):377-388.

41. Lechner MG, Liebertz DJ, Epstein AL. Characterization of cytokine-induced myeloid-derived suppressor cells from normal human peripheral blood mononuclear cells. *J Immunol*. 2010;185(4):2273-2284.

42. Millrud CR, Bergenfelz C, Leandersson K. On the origin of myeloid-derived suppressor cells. *Oncotarget*. 2017;8(2):3649-3665.

43.	Luyckx A, Schouppe E, Rutgeerts O, et al. G-CSF stem cell mobilization in human donors induces polymorphonuclear and mononuclear myeloid-derived suppressor cells. *Clin Immunol*. 2012;143(1):83-87.

44.	Andrlova H, van den Brink MRM, Markey KA. An Unconventional View of T Cell Reconstitution After Allogeneic Hematopoietic Cell Transplantation. *Front Oncol*. 2020;10:608923.

45.	Godfrey DI, Le Nours J, Andrews DM, Uldrich AP, Rossjohn J. Unconventional T Cell Targets for Cancer Immunotherapy. *Immunity*. 2018;48(3):453-473.

46.	Kong Y, Zhu L, Schell TD, et al. T-Cell Immunoglobulin and ITIM Domain (TIGIT) Associates with CD8+ T-Cell Exhaustion and Poor Clinical Outcome in AML Patients. *Clin Cancer Res*. 2016;22(12):3057-3066.

47.	Stamm H, Klingler F, Grossjohann EM, et al. Immune checkpoints PVR and PVRL2 are prognostic markers in AML and their blockade represents a new therapeutic option. *Oncogene*. 2018;37(39):5269-5280.

48.	Valhondo I, Hassouneh F, Lopez-Sejas N, et al. Characterization of the DNAM-1, TIGIT and TACTILE Axis on Circulating NK, NKT-Like and T Cell Subsets in Patients with Acute Myeloid Leukemia. *Cancers (Basel)*. 2020;12(8).

49.	Minnie SA, Kuns RD, Gartlan KH, et al. Myeloma escape after stem cell transplantation is a consequence of T-cell exhaustion and is prevented by TIGIT blockade. *Blood*. 2018;132(16):1675-1688.

50.	Fleischhauer K, Shaw BE. HLA-DP in unrelated hematopoietic cell transplantation revisited: challenges and opportunities. *Blood*. 2017;130(9):1089-1096.

51.	Chakraverty R, Eom HS, Sachs J, et al. Host MHC class II+ antigen-presenting cells and CD4 cells are required for CD8-mediated graft-versus-leukemia responses following delayed donor leukocyte infusions. *Blood*. 2006;108(6):2106-2113.

52.	Stevanovic S, Griffioen M, Nijmeijer BA, et al. Human allo-reactive CD4+ T cells as strong mediators of anti-tumor immunity in NOD/scid mice engrafted with human acute lymphoblastic leukemia. *Leukemia*. 2012;26(2):312-322.

53.	Herr W, Eichinger Y, Beshay J, et al. HLA-DPB1 mismatch alleles represent powerful leukemia rejection antigens in CD4 T-cell immunotherapy after allogeneic stem-cell transplantation. *Leukemia*. 2017;31(2):434-445.

54.	Highfill SL, Rodriguez PC, Zhou Q, et al. Bone marrow myeloid-derived suppressor cells (MDSCs) inhibit graft-versus-host disease (GVHD) via an arginase-1-dependent mechanism that is up-regulated by interleukin-13. *Blood*. 2010;116(25):5738-5747.

55.	Bruce DW, Kolupaev O, Laurie SJ, et al. Third-party type 2 innate lymphoid cells prevent and treat GI tract GvHD. *Blood Adv*. 2021;5(22):4578-4589.

56.	Yew PY, Alachkar H, Yamaguchi R, et al. Quantitative characterization of T-cell repertoire in allogeneic hematopoietic stem cell transplant recipients. *Bone Marrow Transplant*. 2015;50(9):1227-1234.

57.	Schultze-Florey CR, Kuhlmann L, Raha S, et al. Clonal expansion of CD8+ T cells reflects graft-versus-leukemia activity and precedes durable remission following DLI. *Blood Adv*. 2021;5(21):4485-4499.

58.	Uhl FM, Chen S, O'Sullivan D, et al. Metabolic reprogramming of donor T cells enhances graft-versus-leukemia effects in mice and humans. *Sci Transl Med*. 2020;12(567).

59.	McCurdy SR, Radojcic V, Tsai HL, et al. Signatures of GVHD and relapse after posttransplant cyclophosphamide revealed by immune profiling and machine learning. *Blood*. 2022;139(4):608-623.

Figure 1. Longitudinal changes in the immunoregulatory landscape after allo-HSCT

(**A**) Thirty-seven patients with AML/MDS were included in the longitudinal cohort. PBMCs were collected at months 3, M6 and M12 after transplantation and analyzed by mass-cytometry. Twenty healthy donors were also analyzed. (**B**) Unsupervised cell clustering analysis by FlowSOM, with 18 indicated relevant metaclusters. (**C**) Principal component analysis (using FlowSOM data) of all tested samples from patients at indicated time points (M3, n=34; M6, n=31; M12, n=33) and from healthy donors (HD). (**D**) Highlight of cell clusters showing significant longitudinal variations between indicated time points. (**E-F**) Frequencies among PBMCs of cell metaclusters decreasing (**E**) or increasing (**F**) over time. (**G-H**) Volcano plots showing changes between M3 and M6 (**G**) and between M6 and M12 (**H**) in immune parameters assessed by classical manual gating. Significant parameters with │percent change│ > 15% are annotated (% cell population is among total CD45$^+$ live cells, or among a parent cell subset when indicated by "/subset").
P-values correspond to Wilcoxon signed-rank tests. *p <0.05; **p<0.01; ***p<0.001. MC: metacluster.

Figure 2. Persistent alterations in the immunoregulatory landscape at M12 after allo-HSCT

(**A-B**) Frequencies of cell metaclusters (FlowSOM) among PBMCs from patients at month 12 (M12) after transplantation were compared to those of healthy donors. Six out of 18 metaclusters were significantly decreased (A) and one was increased (B). Mann-Whitney tests: *p <0.05; **p<0.01; ***p<0.001; ****p<0.0001. (C) Each immune cell subsets (% cell subset is among total CD45$^+$ live cells, or among a parent cell subset when indicated by "/subset") assessed by classical manual gating was also compared between patients at M12 and healthy donors. Significant (Mann-Whitney tests) parameters are annotated. (D) Altered expression of immunoregulatory molecules in indicated T and NK cell subsets. Color circles indicate significantly increased (red) or decreased (gray) median expression of the regulatory molecules in patients at M12 post-HSCT compared to healthy donors.

Figure 3. Immune parameters associated to late relapse in the longitudinal cohort

(**A**) Principal component analysis (using FlowSOM data) of last available samples from patients with (n=12) or without (n=25) subsequent tumor relapse, as well as of healthy donors. (**B**) Frequencies of cell metaclusters (FlowSOM) in last available samples were compared between patients with or without subsequent tumor relapse. Two out of 18 metaclusters were significantly decreased in patients with subsequent relapse, and one metacluster tended to be increased. These 2 indicated metaclusters are shown here, while other metaclusters (similar in both groups) are shown in suppl. Fig. 3B. *p <0.05 (Mann-Whitney test). (**C**) Volcano plots showing differences between patients with and without relapse in immune parameters at last available time point assessed by classical manual gating. P-values correspond to Mann-Whitney tests. Parameters significantly different between both groups are annotated (% cell population is among total CD45$^+$ live cells, or among a parent cell subset when indicated by "/subset").

Figure 4. Inhibitory receptors expression on T cells associate with subsequent AML tumor relapse in the cross-sectional cohort

(**A**) PBMCs from 40 AML patients with (n=20) and without (n=20) documented subsequent tumor relapse were collected at month 3 after transplantation and analyzed by mass cytometry. (**B**) Unsupervised cell clustering of the T-cell compartment was performed using FlowSOM. (**C**) Volcano plots showing differences between patients with and without relapse in frequencies of FlowSOM-generated T-cell clusters. P-values correspond to Mann-Whitney tests. Clusters significantly different between both groups are annotated (% cell cluster is among total CD3$^+$ T cells, or among CD8 or CD4 T cells when indicated). (**D**) Frequencies of identified cell clusters among CD4 or CD8 T cells in relapsing (R) and non-relapsing (NR) patients. (**E**) Heat map showing expression levels of indicated immunoregulatory molecules in relapse-associated cell clusters. (**F**) Expression of CD161, PD-1, TIGIT and BTLA on total and relapse-associated CD4 T-cell clusters. (**G**) Expression of PD-1 and TIGIT on total and relapse-associated CD8 T-cell cluster. (**H-I**) Enrichment in indicated inhibitory receptors positivity or expression density (median metal intensity, MMI) in relapse-associated clusters relative to total CD4 (H) or CD8 (I) T cells. (**J**) Frequencies of combined "TIGIT clusters" (C25+C26) or "CD161 clusters" (C22+C26) in relapsing (R) and non-relapsing (NR) patients. Relapse-free survival (RFS) assessed using the Kaplan-Meier approach in patients with high (> median) versus low (< median) frequencies of indicated cell clusters are shown in right panels. P-values corresponding to Mann-Whitney or to log-rank tests are indicated to compare cluster frequencies and RFS, accordingly.

Figure 5. Characterization and clinical relevance of CD161$^+$ and TIGIT$^+$ CD4 T cells

(**A**) Representative gating of CD161$^+$, TIGIT$^+$ or PD-1$^+$ CD4 T cells (after exclusion of Treg and MAIT cells). (**B**) Percentage of cells (non-Treg/non-MAIT) expressing CD161, TIGIT, at least CD161 or TIGIT (Boolean gating), or PD-1, among total CD4 T cells from healthy donors (n=20), or from patients (at month 3 after allo-HSCT) with persistent remission (n=20) or with subsequent tumor relapse (n=20). (**C**) Uniform Manifold Approximation and Projection (UMAP) plots showing total CD4 T cells clustering. Indicated cell subsets (from manual gating) are colored while other ungated CD4 T cells are shown in grey (left panel); and expression levels of CD161, TIGIT and PD-1 are depicted (right panels), showing poor overlap between CD161$^+$ and TIGIT$^+$ cells, but strong overlap between TIGIT$^+$ and PD-1^{high} cells. (**D**) Frequencies of cells expressing various inhibitory receptors among the indicated CD4 T-cell subsets. PD-1 cell surface density is also shown (expressed as median metal intensity, MMI) (lower right panel). (**E**) Frequencies of HLA-DR$^+$ or intranuclear Ki-67$^+$ cells among CD161- and TIGIT-expressing CD4 T cells compared to those that do not express CD161 and TIGIT as control (ctrl). (**F**) Frequencies of CD161$^+$ as well as TIGIT$^+$ CD4 T cells were compared with regard to sex and various clinical parameters, i.e. conditioning regimen, donor type, CMV reactivation and acute GVHD. RIC: reduced intensity conditioning; MAC: myeloablative conditioning; MRD: matched related donor; MUD: matched unrelated donor. (**G**) FlowSOM clustering of PBMCs from the 40 patients at M3 post-HSCT was performed based on lineage-defining markers (suppl. Fig. 4). Left panel: frequencies of cluster 34 (corresponding to CD161$^+$ CD4 T cells) among CD4 T cells, in non-relapsing and relapsing patients. Right panel: relapse-free survival (RFS) assessed using the Kaplan-Meier approach in patients with high (> 22%) versus low (< 22%) frequencies of C34 in CD4 T cells. Censored patients are represented by symbols. P-values from Mann-Whitney (panels B, F, G), Wilcoxon (panel E) or log-rank (panel G) tests are indicated: *p <0.05; **p<0.01; ***p<0.001; ****p<0.0001.

Table 1: Patients' characteristics in the longitudinal cohort

Patient Characteristics	All patients. N=37 Median [IQR] or N (%)	No relapse. N=25 Median [IQR] or N (%)	Relapse. N=12 Median [IQR] or N (%)	p-value
Age at transplant, years	51.5 [35.4-61.2]	47.0 [33.9-60.0]	54.0 [37.7-62.8]	0.40
Sex				1
Female	17 (46)	12 (48)	5 (42)	
Male	20 (54)	13 (52)	7 (58)	
Diagnosis				0.12
AML	26 (70)	20 (80)	6 (50)	
MDS	11 (30)	5 (20)	6 (50)	
ELN classification (AML)				0.74
Favorable	7 (27)	6 (30)	1 (17)	
Intermediate	10 (38)	8 (40)	2 (33)	
Adverse	9 (35)	6 (30)	3 (50)	
Number of pre-transplant treatment				0.73
0	2 (5)	2 (8)	0 (0)	
1	23 (62)	14 (56)	9 (75)	
≥ 2	12 (32)	9 (36)	3 (25)	
Disease status at transplant				0.11
CR1	17 (46)	13 (52)	4 (33)	
CR≥2	10 (27)	8 (32)	2 (17)	
No CR	10 (27)	4 (16)	6 (50)	
Conditioning				**0.01**
Myeloablative	14 (38)	13 (52)	1 (8)	
Reduced intensity	22 (59)	12 (48)	10 (83)	
Sequential	1 (3)	0 (0)	1 (8)	
Serotherapy	20 (54)	12 (48)	8 (67)	0.32
Donor				0.58
Related	18 (49)	11 (44)	7 (58)	
Matched unrelated	16 (43)	11 (44)	5 (42)	
Mismatched unrelated	3 (8)	3 (12)	0 (0)	
Stem cells source				0.11
Bone marrow	1 (3)	1 (4)	0 (0)	
Peripheral blood	34 (92)	24 (96)	10 (83)	
Umbilical cord blood	2 (5)	0 (0)	2 (17)	
GVHD prophylaxis				0.12
CSA	1 (3)	1 (4)	0 (0)	
CSA + MMF	19 (51)	10 (40)	9 (75)	
CSA + MTX	17 (46)	14 (56)	3 (25)	
Acute GVHD all grades	18 (49)	15 (60)	3 (25)	0.08
Acute GVHD grade III/IV	3 (8)	3 (12)	0 (0)	0.54
Chronic GVHD	10 (27)	9 (36)	1 (8)	0.12
None	3 (30)	3 (33)	0 (0)	
moderate	5 (50)	4 (44)	1 (100)	
extensive	2 (20)	2 (22)	0 (0)	
CMV reactivation	6 (16)	4 (16)	2 (17)	1
Death	8 (22)	1 (4)	7 (58)	**0.0005**
Cause of death				
GVHD	1 (13)	1 (4)	0 (0)	**0.0005**
Relapse	7(87)	0 (0)	7 (58)	

Abbreviations: AML: acute myeloid leukemia ; CMV: cytomegalovirus ; CSA: cyclosporine ; ELN: European LeukemiaNet ; GVHD: graft versus host disease ; MMF: mycophenolate mofetil ; MTX: methotrexate ; CR: Complete response.

Table 2: Patients' characteristics in the cross-sectional cohort

Patient Characteristics	All patients. N=40 Median [IQR] or N (%)	No relapse. N=20 Median [IQR] or N (%)	Relapse. N=20 Median [IQR] or N (%)	p-value
Age at transplant, years	52.5 [43-59]	52.5 [45.5-60.5]	52.5 [38.7-58.5]	0.51
Sex				1
Female	21 (52)	11 (55)	10 (50)	
Male	19 (48)	9 (45)	10 (50)	
ELN classification				0.65
Favorable	5 (12,5)	2 (10)	3 (15)	
Intermediate	18 (45)	10 (50)	8 (40)	
Adverse	17 (42.5)	8 (40)	9 (45)	
Number of pre-transplant treatment				0.16
1	29 (72)	17 (85)	12 (60)	
≥ 2	11 (28)	3 (15)	8 (40)	
Disease status at transplant				0.10
CR1	27 (67)	17 (85)	10 (50)	
CR≥2	8 (20)	2 (10)	6 (30)	
No CR	5 (13)	1 (5)	4 (20)	
Conditioning				0.46
Myeloablative	9 (22,5)	5 (25)	4 (20)	
Non myeloablative	3 (7.5)	2 (10)	1 (5)	
Reduced intensity	25 (62,5)	13 (65)	12 (60)	
Sequential	3 (7.5)	0 (0)	3 (15)	
Serotherapy	32 (80)	16 (80)	16 (80)	1
Donor				0.79
Related	19 (47.5)	10 (50)	9 (45)	
Matched unrelated	18 (45)	8 (40)	10 (50)	
Mismatched unrelated	3 (7.5)	2 (10)	1 (5)	
Stem cells source				0.22
Bone marrow	2 (5)	0 (0)	2 (10)	
Peripheral blood	37 (92,5)	20 (100)	17 (85)	
Umbilical cord blood	1 (2.5)	0 (0)	1 (5)	
GVHD prophylaxis				0.17
CSA	2 (5)	0 (0)	2 (10)	
CSA + MMF	28 (70)	13 (65)	15 (75)	
CSA + MTX	10 (25)	7 (35)	3 (15)	
Acute GVHD all grades	14 (35)	8 (40)	6 (30)	0.74
Acute GVHD grade III/IV	7 (17.5)	4 (20)	3 (15)	1
Chronic GVHD	12 (30)	9 (45)	3 (15)	0.08
None	2 (5)	2 (22)	0 (0)	
moderate	4 (10)	3 (15)	1 (5)	
extensive	6 (15)	4 (20)	2 (10)	
CMV reactivation	7 (17.5)	3 (15)	4 (20)	1
Death	22 (55)	3 (15)	19 (95)	**4.10^{-7}**
Cause of death				
GVHD	1 (2.5)	1 (5)	0 (0)	
Relapse	18 (45)	0 (0)	18 (90)	
Secondary cancer	1 (2.5)	1 (5)	0 (0)	
Toxicity	1 (2.5)	1 (5)	0 (0)	

Abbreviations: AML: acute myeloid leukemia ; CMV: cytomegalovirus ; CSA: cyclosporine ; ELN: European LeukemiaNet ; GVHD: graft versus host disease ; MMF: mycophenolate mofetil ; MTX: methotrexate ; CR: Complete response.

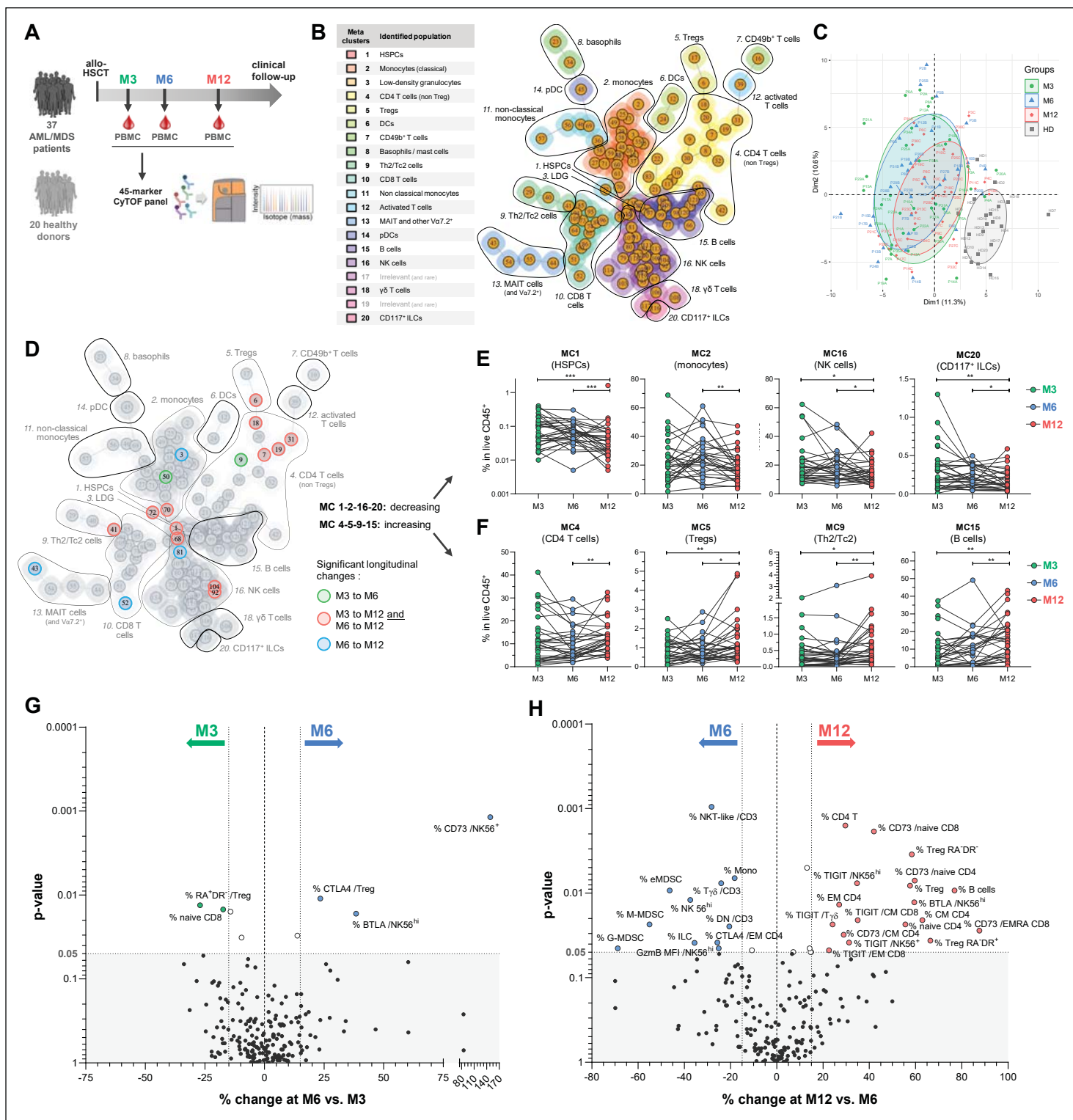**Figure 1 – Longitudinal changes in the immunoregulatory landscape after allo-HSCT**

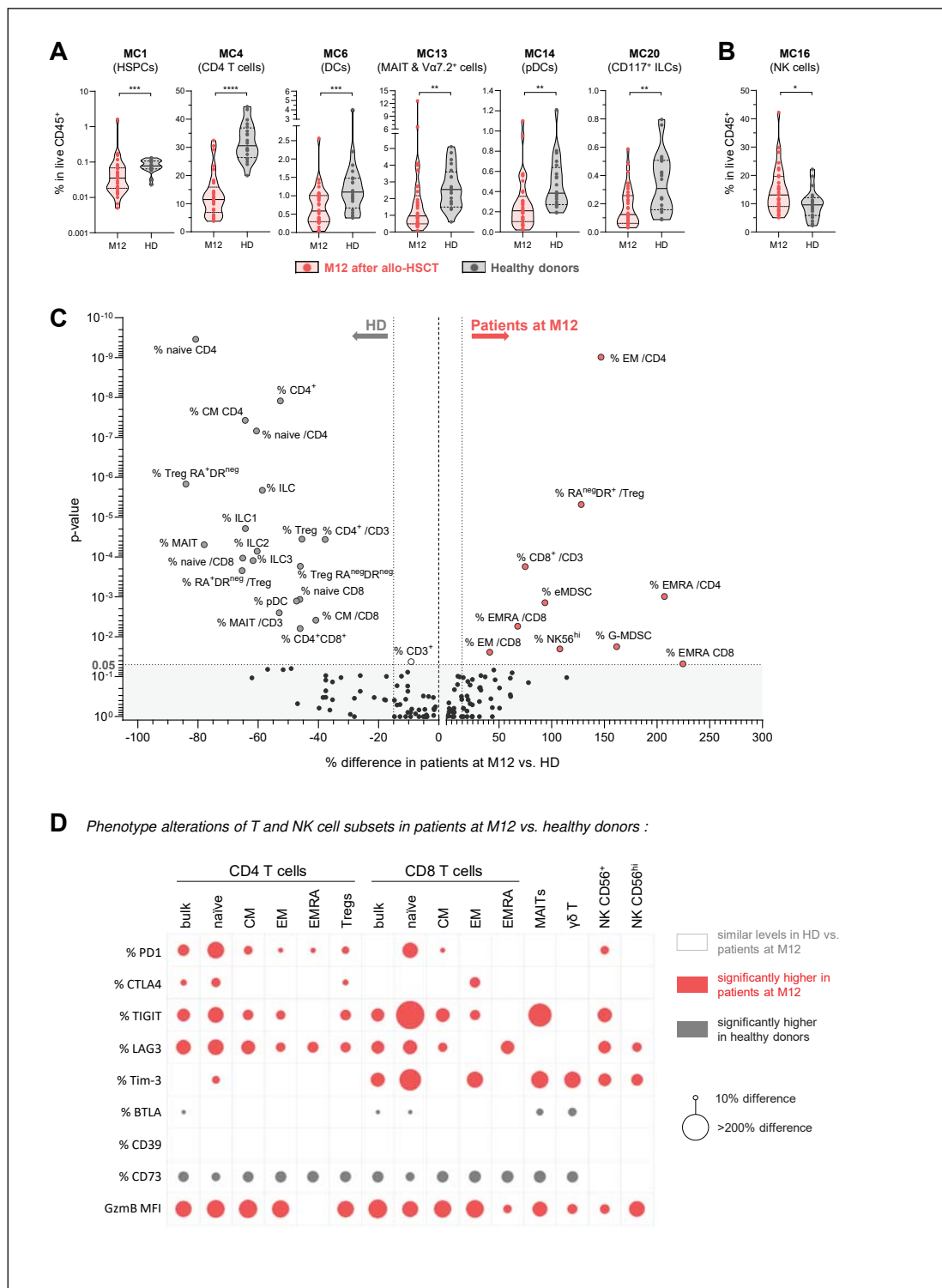**Figure 2 – Persistent alterations in the immunoregulatory landscape at M12 after allo-HSCT**

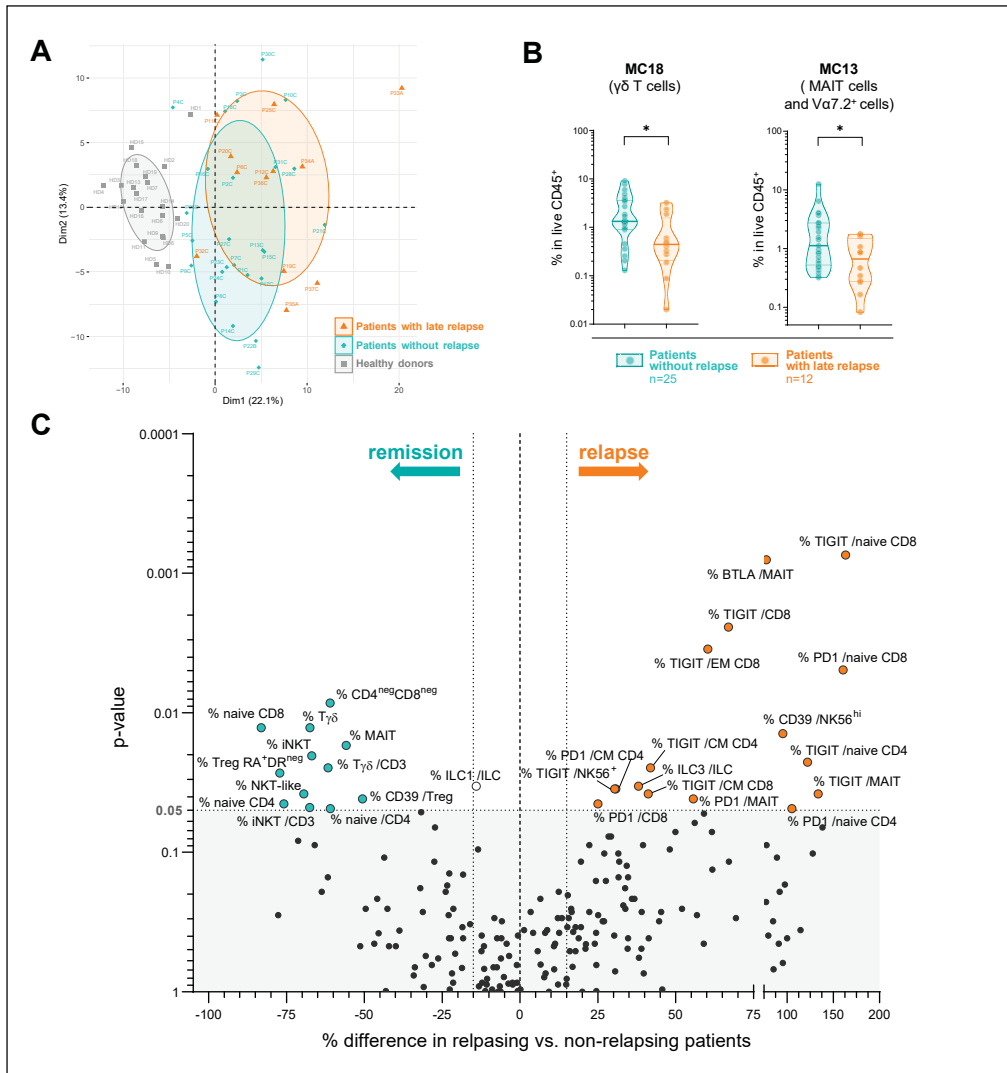**Figure 3 – Immune parameters associated to late relapse in the longitudinal cohort**

Figure 4 – Inhibitory receptors expression on T cells associate with subsequent AML tumor relapse in the cross-sectional cohort
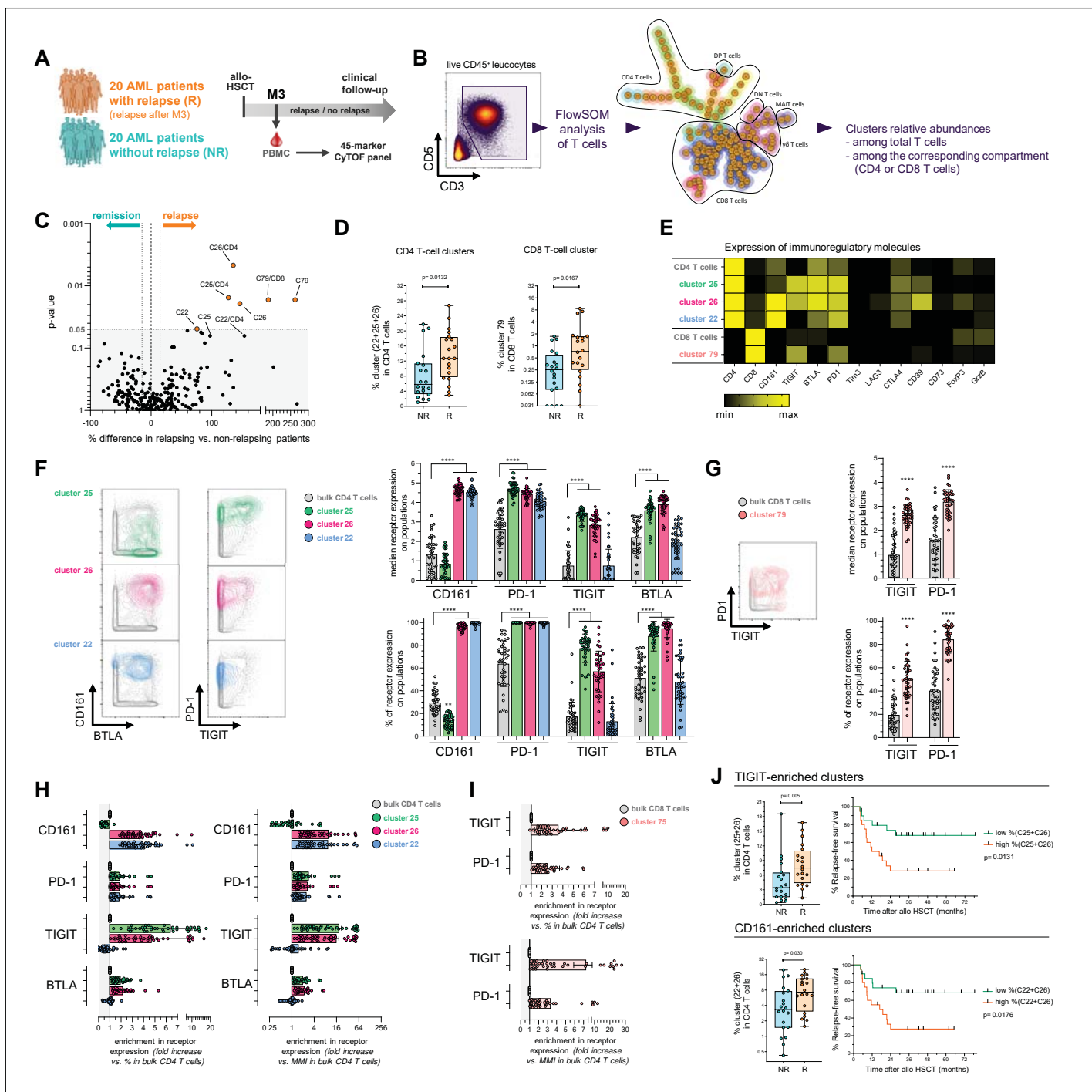
Figure 5 – Characterization and clinical relevance of CD161+ and TIGIT+ CD4 T cells